MAD/PH/237
February 1985

MONOJETS AND ANOMALOUS LEPTON-$\not{p}_T$-JET EVENTS IN THE STANDARD MODEL

Jean-René Cudell, Francis Halzen and Ken-ichi Hikasa
Physics Department, University of Wisconsin, Madison, Wisconsin 53706

ABSTRACT

We systematically investigate the uncertainties in computing the production of $W^{\pm}, Z$ with large transverse momentum in $p\bar{p}$ interactions. We argue that the rates for "anomalous" lepton-$\not{p}_T$-jet events can be consistent with the standard model prediction for the process $\bar{p}p \to W(\to \ell\nu)$ + gluons. As a result we also predict enhanced "monojet" cross sections from $\bar{p}p \to Z(\to \nu\bar{\nu})$ + gluons, although the overall rate is still somewhat low. This discrepancy would be remedied if there exist more than three light neutrinos, as is predicted by some family-unifying theories.

The discovery[1,2] of anomalous events with missing transverse momentum ($\not{p}_T$) + jets and lepton ($\ell = e,\mu$) + $\not{p}_T$ + jets at the CERN $p\bar{p}$ collider has recently withstood the test of higher statistics.[3,4] These events have been regarded as an indication of "new physics". However, such events occur in the standard model as a result of the production of weak bosons in association with gluons: $Z(\to \nu\bar{\nu})$ + gluons and $W(\to \ell\nu)$ + gluons.

The first process qualitatively reproduces the features of so-called monojet events.[1,4] Not only the event structure, but also the kinematic features of monojets can be mimicked. As a function of the jet transverse momentum p_T the monojet cross section shows the usual QCD-type falloff at large p_T as well as a sharp cutoff at low p_T (typically $p_T \leq 30$ GeV) because of detection efficiency. A $Z \to \nu\bar{\nu}$ decay is indeed unobservable at $p_T = 0$, as there is no transverse momentum imbalance. The detector only reaches a 90% detection efficiency around $p_T \simeq 35$ GeV. As a kinematic reflection, the ($\not{p}_T$,jet) invariant mass also rises sharply in the 110 ~ 120 GeV region; at larger p_T values it again displays the familiar QCD suppression.

"Monojets" is of course a misnomer, as for larger p_T values two or three jets are almost as likely to balance the Z's transverse momentum as a single jet. This is clearly illustrated by existing $Z \to \ell\bar{\ell}$ data[5] and is certainly expected from a theoretical point of view. A completely parallel discussion can be made for $\ell + \not{p}_T$ + jet events[2,3] with $W \to \ell\nu$ substituted for $Z \to \nu\bar{\nu}$.

The main reason* that these as well as the monojet events are tagged "anomalous" is that their observed rates exceed the predictions of the

*For the monojet events some observed jets have a very low multiplicity; we comment on this further on.

standard model. Typically, event rates exceed existing calculations by "a factor". It is the purpose of this letter to systematically investigate the intrinsic ambiguities of standard model calculations for the production and decay of weak intermediate bosons.

The uncertainty in the evaluation of the standard model background has two main sources: (i) the branching ratio $Z \to \nu\bar{\nu}$ which depends on the unknown (but constrained[6-8]) number of light neutrinos and (ii) ambiguities in the perturbative calculation of weak boson yields as a function of their transverse momentum. We discuss these in reverse order.

From a theoretical point of view there are two distinct regimes for producing weak bosons: $p_T \ll M_Z$ and $p_T \simeq M_Z$. Calculations exist covering both kinematic regions.[9,10] Calculations in the $p_T \ll M_Z$ region require the resummation of gluon emission and are at best exploratory. Independent of any theoretical questions they are based on "leading logarithm kinematics" where one routinely computes momentum fractions of the partons as $x = M_Z/\sqrt{s}$, whereas exact kinematics dictates $x = (M_Z + p_T)/\sqrt{s}$ $(y = 0)$. Even at $p_T = 15$ GeV this leads to ambiguities in evaluating the parton flux factor $q(x_1)\bar{q}(x_2)$ of order of a factor 2.

At $p_T \simeq M_Z$ the cross sections are determined by leading order perturbation theory from the diagrams $q\bar{q} \to Zg$ and $gq \to Zq$. Here the calculation is straightforward;[11] because of the aforementioned ambiguities in the $p_T \ll M_Z$ region it is however difficult to pinpoint the transition region where leading order perturbation theory becomes reliable. Guided by the results of Refs. 9, 12 we will here assume that gluon resummation does not affect the results for $p_T > 20$ GeV so that related problems can be ignored in the present discussion. Our main results are actually confined to the region $p_T > 30$ GeV.

Uncertainties in the leading order calculation of the large p_T weak boson yields are associated with: (i) uncertainties in the structure functions, (ii) choice of the scale Q^2 of α_s and of the evolution of the structure functions, (iii) higher-order effects, (iv) experimental resolution of $\not{p}_T$ and (v) others*. In order to evaluate the uncertainties connected with (i) and (ii) we performed calculations for a representative collection** of structure functions[13-15] and a range of choices of the evolution scale bounded by p_T^2 and $\hat{s}$, the $q\bar{q}$ subprocess energy. The QCD parameter Λ ranges from 0.2 GeV to 0.4 GeV depending on structure functions. In the absence of higher-order calculations it is indeed impossible to decide on a "best" or "appropriate" choice of Q^2. Our choices are not even exhaustive as, e.g., $Q^2 = p_T^2/4$ might deliver the fastest converging perturbative series.

We next turn to the problem of next-to-leading order corrections. They are known to be sizeable in interactions dominated by $q\bar{q}$-initiated processes[18] such as $\pi N \to (\mu^+\mu^-)X$ and have been partially calculated.[19] They are associated with virtual gluon corrections to $q\bar{q} \to Zg$ and higher-

---

*E.g., we do not consider problems related to the fact that information from nuclear target experiments is used in determining structure functions.

**The structure function of Eichten et al.[16] does not reproduce the ratio $d_v(x)/u_v(x)$ obtained from electron scattering data, and is not suitable for the study here. The cross sections derived from their structure function are, however, close to our results in Figs. 1-2. The structure function proposed by Baier et al.[17] is inappropriate for any electroweak process, because they simply assume $u_v(x) = 2d_v(x)$, which has been excluded by experimental data.

order diagrams such as $q\bar{q} \to Zgg$. An economical description[†] of this correction may be given by

$$\frac{d\sigma}{dp_T^2} \simeq \exp\left[\frac{\alpha_s(p_T^2)}{2\pi} C_F \pi^2\right]\left[\frac{d\sigma}{dp_T^2}\right]_{O(\alpha_s)} , \tag{1}$$

which represents a guess as to how these corrections sum up in higher orders of perturbation theory. Here $C_F = 4/3$. We again repeated all calculations including this factor.

The results so obtained for the W,Z cross section as a function of transverse momentum are shown in Figs. 1, 2. We present the results in differential and integral (cumulative) forms; all calculations fall into the bands shown in the figure. The band roughly spans a factor of 3 which is the cumulative effect of factors 1.25, 1.6 and 1.35, due respectively to the structure functions, the choice of scale and the correction of Eq. (1). The largest cross sections are obtained for the structure functions of Glück et al.,[14] $Q^2 = p_T^2$ and inclusion of the correction of Eq. (1). One might actually favor this choice of scale in $\alpha_s(Q^2)$ and $q(z,Q^2)$ as it directly expresses the fact that the scale of the interaction changes with the transverse momentum of the produced Z. As a consistency check we have computed the production of lepton pairs in $\pi^- N$ interactions.

[†]The multiplicative factor in Eq. (1) is the same as the conjectured exponentiated form[20] of the factor found in the $O(\alpha_s)$ contribution[21] to the process $q\bar{q} \to \gamma^*$. At our energies, it gives a moderate enhancement factor of 1.3 - 1.4 to the cross section. Use of the first two terms of the expansion in α_s $(1 + \pi C_F \alpha_s/2)$ instead of the exponential factor gives only a slight difference.

Although comparison[*] with data[22] is only possible at much smaller values of p_T and $\sqrt{s}$, the confrontation is relevant as it is a $q\bar{q} \to \gamma^* g$ dominated process in a similar range of $M/\sqrt{s}$ and $p_T/\sqrt{s}$ values. Our assumptions fit the πN data rather well, as can be seen from Fig. 3.[**]

In summary, we feel that the bands shown in Figs. 1, 2 should be considered as a representative measure of theoretical uncertainties rather than absolute upper and lower bounds. Nevertheless, we will continue our discussion using the results obtained with the specific set of assumptions yielding the maximal results in Figs. 1, 2.

We discuss the implication of these results for "anomalous" $p\bar{p}$ events next. It is clear from Fig. 2 that 1 ∼ 2 events $W(\to e\nu)$ + jet(s) are expected for $p_T > 30$ GeV and 0.7 events for $p_T > 40$ GeV per integrated luminosity of 100 nb^{-1}. This is consistent with the rate of $\ell + \not{p}_T$ + jet events observed in the most recent UA2 data sample[3] and with the observation of one such event by the UA1 group (event A in Ref. 1; they also have several high-p_T events[4] in the new data). Two of the previous UA2 events[2] might still defy explanation; it is however important at this point to realize that the experimental resolution can strongly affect this type of comparison as one is comparing with a steeply falling distribution. Especially errors on $\not{p}_T$ should be taken into account. They can shift the actual p_T value by 5 ∼ 10 GeV from the measured one, leading to a significant increase of the expected event rate. A comparison of the calculation with the complete sample of $\ell + \not{p}_T$ + jet data is shown in Fig. 4a.

[*]We again investigated a range of π structure functions. The results shown in Fig. 3 are based on the NA3 π structure function of Ref. 22; other choices can modify the calculation by up to a factor 1.5.

[**]See also Ref. 18. The analytic result calculated for a nonsinglet combination in Ref. 19 gives a numerically similar factor as our simple parametrization.

In Fig. 5a we calculated the (W,jet) invariant mass distribution for $p_T > 15$, 30 GeV. Given the low statistics of the data and the relatively large ambiguities in the standard model predictions, definite conclusions will still have to await higher statistics.* It is however clear that our larger cross section predictions are closest to the data. As the ratio of W to Z cross sections is relatively well understood[7,8,10] (see Fig. 6c), this gives us confidence in using the larger Z cross sections for discussing the monojet background. If anything, our expectations might still be on the conservative side, as the data has not been corrected for detection efficiency. This might be a sizeable correction for W's.

We have pointed out already that the monojet data display the qualitative features expected from the process $Z(\rightarrow \nu\bar{\nu})$ + gluon(s). We expect a peak around $p_T \simeq 30$ GeV where the detection efficiency for $Z \rightarrow \nu\bar{\nu}$ turns on. The corresponding (Z,jet) invariant mass** is shown in Fig. 5b for $p_T > 15$, 30 GeV covering again the region where the UA1 detector becomes sensitive to the decay $Z \rightarrow \nu\bar{\nu}$. The distribution looks qualitatively like the monojet data[1,4] with a peak expected in the 100 $\sim$ 120 GeV invariant mass region. This region is of course further populated by $W(\rightarrow \tau\nu)$ + gluon events.

We now turn to the issue of monojet rates. As can be seen from Fig. 2, we expect roughly 2 $\sim$ 10 Z's with $p_T > 30$ GeV per 100 nb^{-1}. For three light neutrinos ($N_\nu = 3$ in Fig. 6) the branching fraction for $Z \rightarrow \nu\bar{\nu}$

---

*The shape of the differential cross section can be predicted more reliably than the absolute value (as seen from Fig. 1), thus providing a sensitive test of the standard model.

**The Z-jet invariant mass is not a measurable quantity in $\not{p}_T$-jet events. However, it can be measured for Z° decaying to $\ell\bar{\ell}$ or jets.

is 0.2. We therefore expect "a few" monojets per 100 nb^{-1}. Although the question of backgrounds is complex, all indications are that the observed rates are higher than predicted by our calculation. There is, however, an intrinsic ambiguity in this calculation related to the number of neutrinos N_ν. E.g., for $N_\nu = 8$ as suggested by some family-unifying theories, the branching ratio $Z \rightarrow \nu\bar{\nu}$ is increased by a factor 2 (see Fig. 6). It is therefore conceivable that the standard model with $N_\nu > 3$ can accommodate the data. Our prediction is compared with data in Fig. 4b assuming $N_\nu = 3$, 8. Such a scenario can be subjected to internal tests using $p\bar{p}$ collider data. Increasing N_ν increases the total width of the Z and the ratio $R = B\sigma(W \rightarrow \ell\nu)/B\sigma(Z \rightarrow \ell\bar{\ell})$ as shown in Fig. 6. For $N_\nu = 8$, $\Gamma_Z \simeq 3.7$ GeV is well within present experimental bounds. R is increased to 11.6 ± 0.7 up from the standard $N_\nu = 3$ value of R = 8.8. Notice that the ratio R is predicted with an accuracy far superior to that for individual W,Z cross sections because most uncertainties in the calculation (except that from structure functions) cancel in the ratio.[7,10] Obviously the rates for Z production with large p_T can be checked using the $Z \rightarrow \ell\bar{\ell}$ decay mode.*

We conclude with a comment. If monojets are a signature of $N_\nu > 3$, they might be the first glimpse of a rich structure to be uncovered by the collider in the near future. E.g., in the much heralded GUT of family unity O(18)[24], eight neutrinos below M_Z could be the only witnesses below M_Z of a rich generation structure above M_Z. Some of these neutrinos could have masses of a few GeV and very long lifetimes. They could lead to a different type of monojet event with one neutrino escaping the detector

---

*This is another way to count the number of neutrinos. See also Ref. 23.

and the other one decaying hadronically into a thin jet. The O(18) theory predicts[24] one more and another four "mirror" generations of quarks and leptons of weak-scale masses and some of them are likely to have a mass of about 100 GeV.[25] These particles would be discovered by the Fermilab or the upgraded CERN colliders.

Acknowledgments

We thank J. Bagger, D. Cline, J. Cortes, F. Herzog, W. Long, P. Minkowski, M. Mohammadi and J. Rholf for discussions.

This research was supported in part by the University of Wisconsin Research Committee with funds granted by the Wisconsin Alumni Research Foundation, and in part by the Department of Energy under contract DE-AC02-76ER00881.

REFERENCES

1. UA1 Collaboration, G. Arnison et al., Phys. Lett. 139B, 115 (1984).
2. UA2 Collaboration, P. Bagnaia et al., Phys. Lett. 139B, 105 (1984).
3. J. R. Hansen, talk at the Aspen Winter Physics Series, "Collider Physics at Ultrahigh Energies", Aspen, Colorado, January, 1985.
4. M. Mohammadi, V. Vuillemin, talk at Aspen Winter Physics Series, Aspen, Colorado, January, 1985.
5. UA1 Collaboration, G. Arnison et al., Phys. Lett. 126B, 398 (1983); 147B, 241 (1984); S. Geer, CERN report CERN-EP/84-160, to be published in Particles and Fields - 1984, Santa Fe, New Mexico (November, 1984).
6. F. Halzen and M. Mursula, Phys. Rev. Lett. 51, 857 (1983); D. Cline and J. Rholf, unpublished.
7. K. Hikasa, Phys. Rev. D 29, 1939 (1984).
8. N. G. Deshpande, G. Eilam, V. Barger and F. Halzen, Madison report MAD/PH/235 (1985).
9. F. Halzen, A. D. Martin and D. M. Scott, Phys. Lett. 112B, 160 (1982).
10. G. Altarelli, R. K. Ellis, M. Greco and G. Martinelli, Nucl. Phys. B 246, 12 (1984).
11. F. Halzen and D. M. Scott, Phys. Lett. 78B, 318 (1978).
12. P. Aurenche and R. Kinnunen, Phys. Lett. 135B, 493 (1984); P. Minkowski, Phys. Lett. 139B, 431 (1984).
13. D. W. Duke and J. F. Owens, Phys. Rev. D 30, 49 (1984).
14. M. Glück, E. Hoffmann and E. Reya, Z. Phys. C 13, 119 (1982).
15. A. J. Buras and K.J.F. Gaemers, Nucl. Phys. B 132, 249 (1978); J. F. Owens and E. Reya, Phys. Rev. D 17, 3003 (1978).
16. E. Eichten, I. Hinchliffe, K. Lane and C. Quigg, Rev. Mod. Phys. 56, 579 (1984).

17. R. Baier, J. Engels and B. Petersson, Z. Phys. C 8, 265 (1979).

18. F. Halzen and D. M. Scott, Phys. Rev. D 24, 2433 (1981).

19. R. K. Ellis, G. Martinelli and R. Petronzio, Phys. Lett. 104B, 45 (1981); Nucl. Phys. B 211, 106 (1983).

20. G. Parisi, Phys. Lett. 90B, 295 (1980); G. Curci and M. Greco, Phys. Lett. 92B, 175 (1980).

21. G. Altarelli, R. K. Ellis and G. Martinelli, Nucl. Phys. B 143, 511 (1978); B 146, 544 (E) (1978); B 147, 461 (1979); J. Kubar-Andre and F. E. Paige, Phys. Rev. D 19, 221 (1979); K. Harada, T. Kaneko and N. Sakai, Nucl. Phys. B 155, 169 (1979); B 167, 545 (E) (1980); J. Abad and B. Humpert, Phys. Lett. 80B, 286 (1979); J. Abad, B. Humpert and W. L. van Neerven, Phys. Lett. 83B, 371 (1979).

22. NA3 Collaboration, J. Badier et al., Phys. Lett. 117B, 372 (1982).

23. M. Chaichian and M. Hayashi, Phys. Rev. D 30, 243 (1984).

24. J. Bagger and S. Dimopoulos, Nucl. Phys. B 244, 247 (1984).

25. J. Bagger, S. Dimopoulos and E. Massó, SLAC report SLAC-PUB-3437 (1984).

FIGURE CAPTIONS

Fig. 1. Transverse momentum distribution of W,Z in $p\bar{p}$ interactions with $\sqrt{s}$ = 630 GeV. The W scale has been shifted upwards by a factor 10. The theoretical errors (not necessarily upper/lower limits) are described in the text.

Fig. 2. Integral distributions corresponding to the transverse momentum distributions shown in Fig. 1. The scale on the right-hand side gives the number of W,Z events passing a minimum p_T cut p_T^0 for an integrated luminosity of 100 nb^{-1}. Predictions for $\sqrt{s}$ = 540 and 630 GeV are shown separately.

Fig. 3. A calculation of the transverse momentum distribution of lepton pairs in πN interactions, based on identical assumptions to those resulting in the largest W,Z cross sections shown in Figs. 1, 2, is compared to the data of Ref. 22. The discrepancy with the low energy data can be accounted for by the intrinsic transverse momentum of the colliding partons.[18,19]

Fig. 4. Comparison of ℓ-$\not{p}_T$-jets and $\not{p}_T$-jet(s) data of Refs. 1-4, with the standard model predictions for $\sqrt{s}$ = 630 GeV. The event rate was obtained by normalizing each event to the luminosity of the sample in which it has been observed. No corrections for detection efficiency have been applied. We assumed a branching ratio $B(W \to \ell\nu) = 1/12$ in Fig. 4a and $B(Z \to \nu\bar{\nu}) = 0.2, 0.4$ in Fig. 5b. This corresponds to

the standard model with three (solid line) and eight (dashed line) light neutrinos. Also shown in Fig. 5b is the Z transverse momentum distribution shifted by 8 GeV in order to illustrate the importance of errors on the $\not{p}_T$ measurement. A Gaussian experimental resolution of 10 GeV for the missing p_T would increase the apparent cross section resulting in a shift in scale by $\sim$ 5 GeV.

Fig. 5. Invariant mass of the W-jet and Z-jet system corresponding to the larger transverse momentum distribution shown in Fig. 1. Separately shown are the result for a minimum transverse momentum of the jet (or W,Z) of 15, 30 GeV.

Fig. 6. Standard model predictions for the total width, the branching ratio into neutrinos of the Z boson and the number of $W^{\pm}$ to Z^0 events observed in a definite $\ell\nu, \ell\bar{\ell}$ leptonic mode as a function of the number of light neutrinos. Errors in Fig. 6c have been obtained using the same procedure leading to the errors in Fig. 1. The error for the ratio is much smaller than that for the individual cross sections.

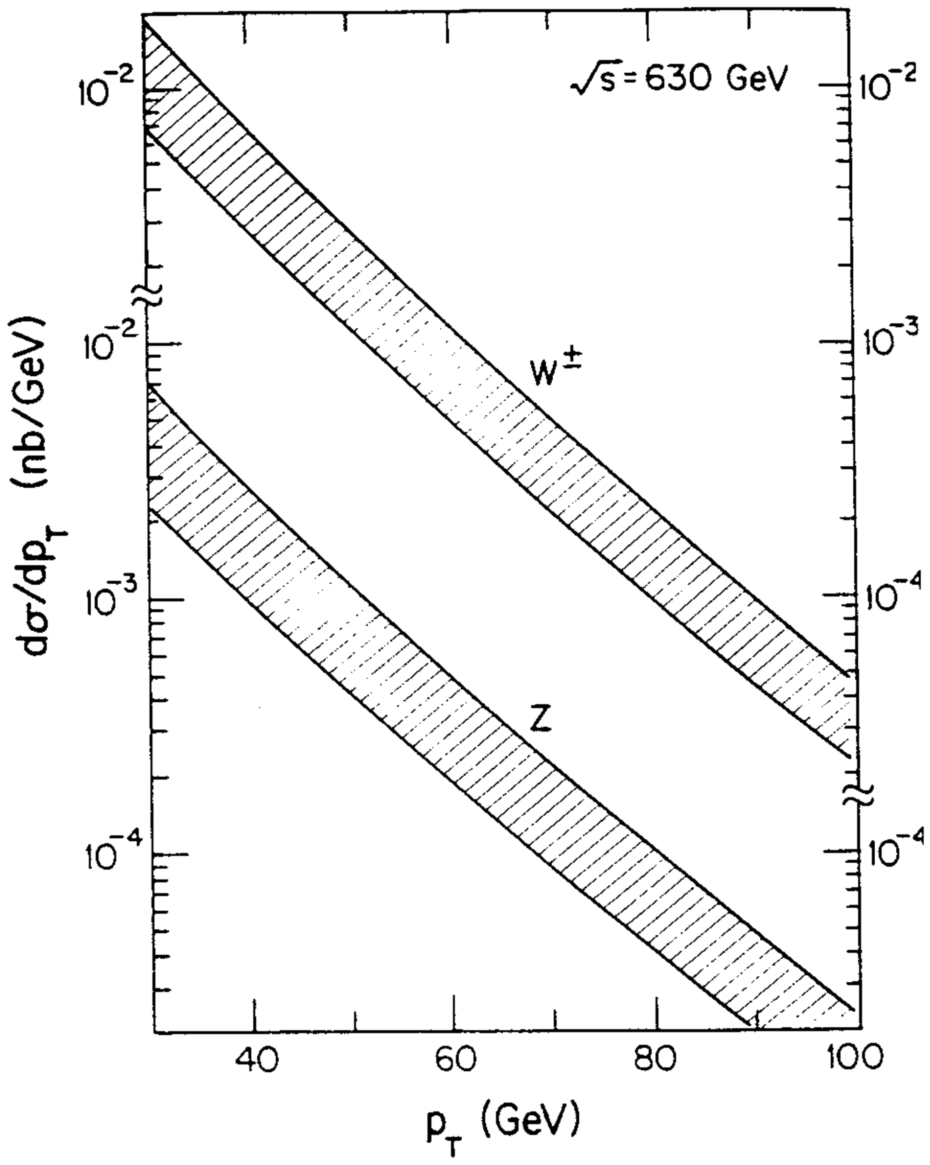

Fig. 1

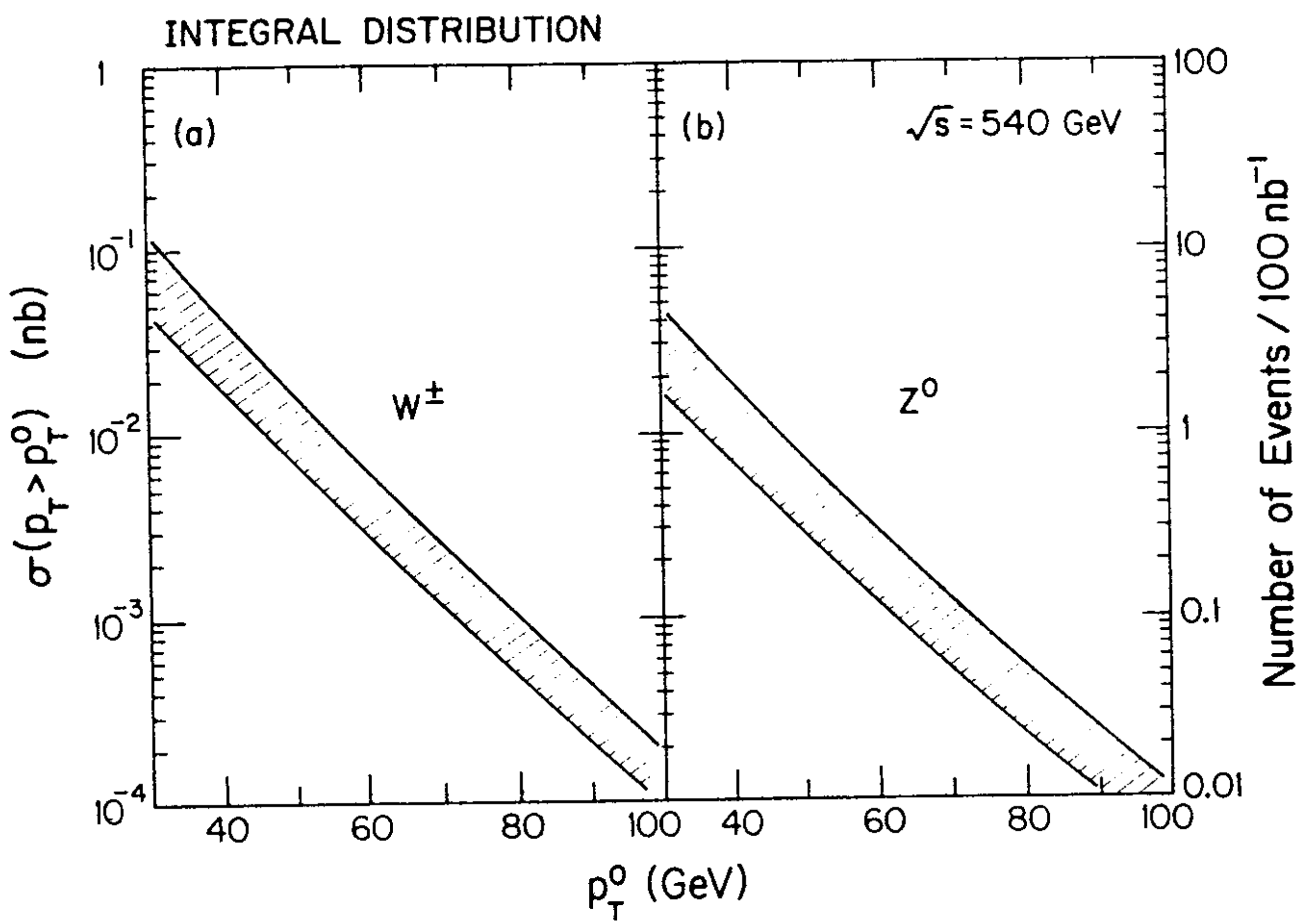
INTEGRAL DISTRIBUTION
(a)
(b)
√s = 540 GeV
W±
Z0
σ(pT > pT0) (nb)
Number of Events / 100 nb-1
pT0 (GeV)
1
10-1
10-2
10-3
10-4
100
10
1
0.1
0.01
40
60
80
100

Fig. 2(a) and (b)

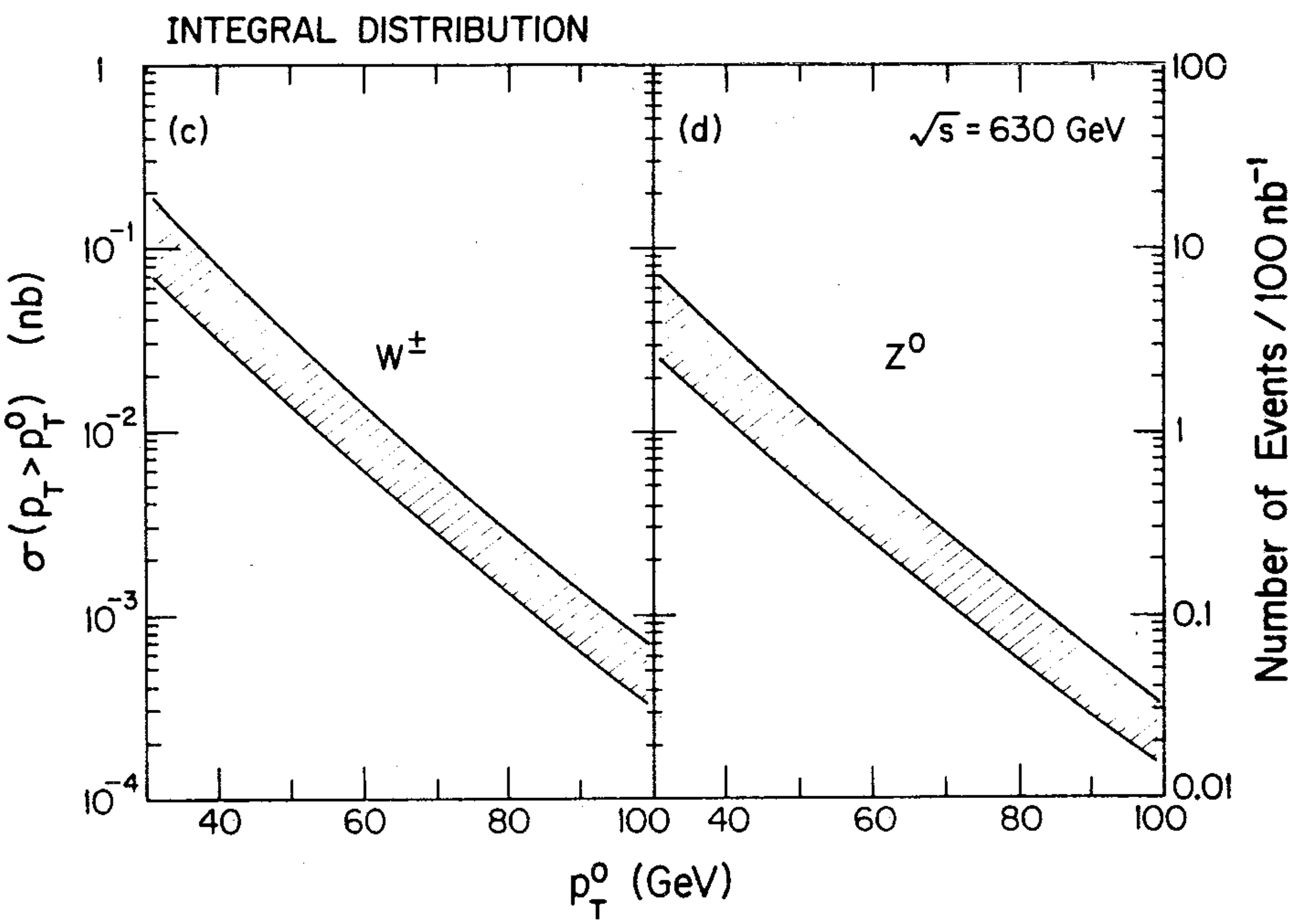

INTEGRAL DISTRIBUTION
(c)
(d)
√s = 630 GeV
W±
Z0
σ(pT > pT0) (nb)
Number of Events / 100 nb-1
pT0 (GeV)
1
10-1
10-2
10-3
10-4
100
10
1
0.1
0.01
40
60
80
100

Fig. 2(c) and (d)

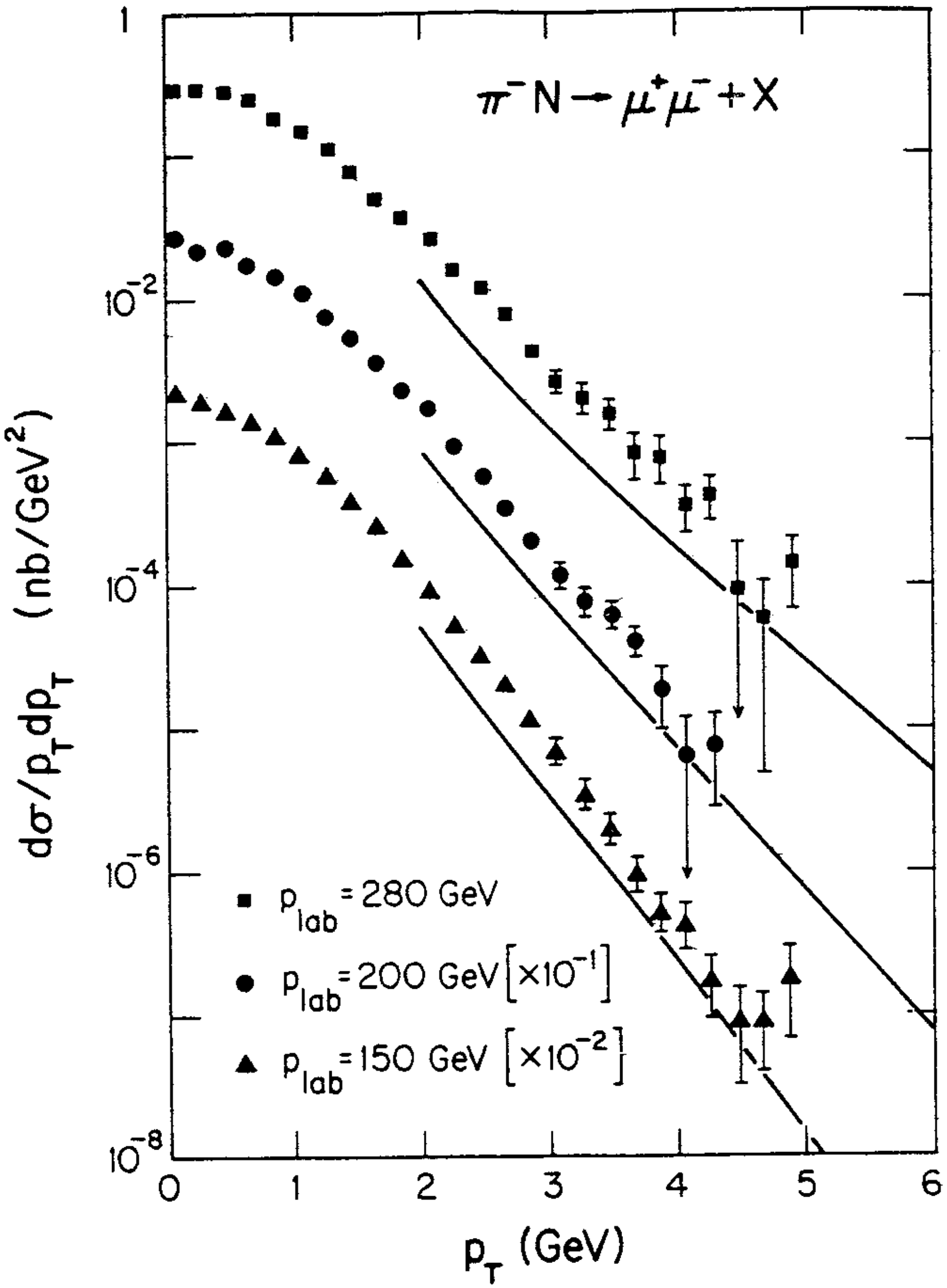

$\pi^- N \rightarrow \mu^+\mu^- + X$
$d\sigma/p_T dp_T$ (nb/GeV^2)
p_T (GeV)
p_{lab} = 280 GeV
p_{lab} = 200 GeV [$\times 10^{-1}$]
p_{lab} = 150 GeV [$\times 10^{-2}$]
1
10^{-2}
10^{-4}
10^{-6}
10^{-8}
0
1
2
3
4
5
6

Fig. 3

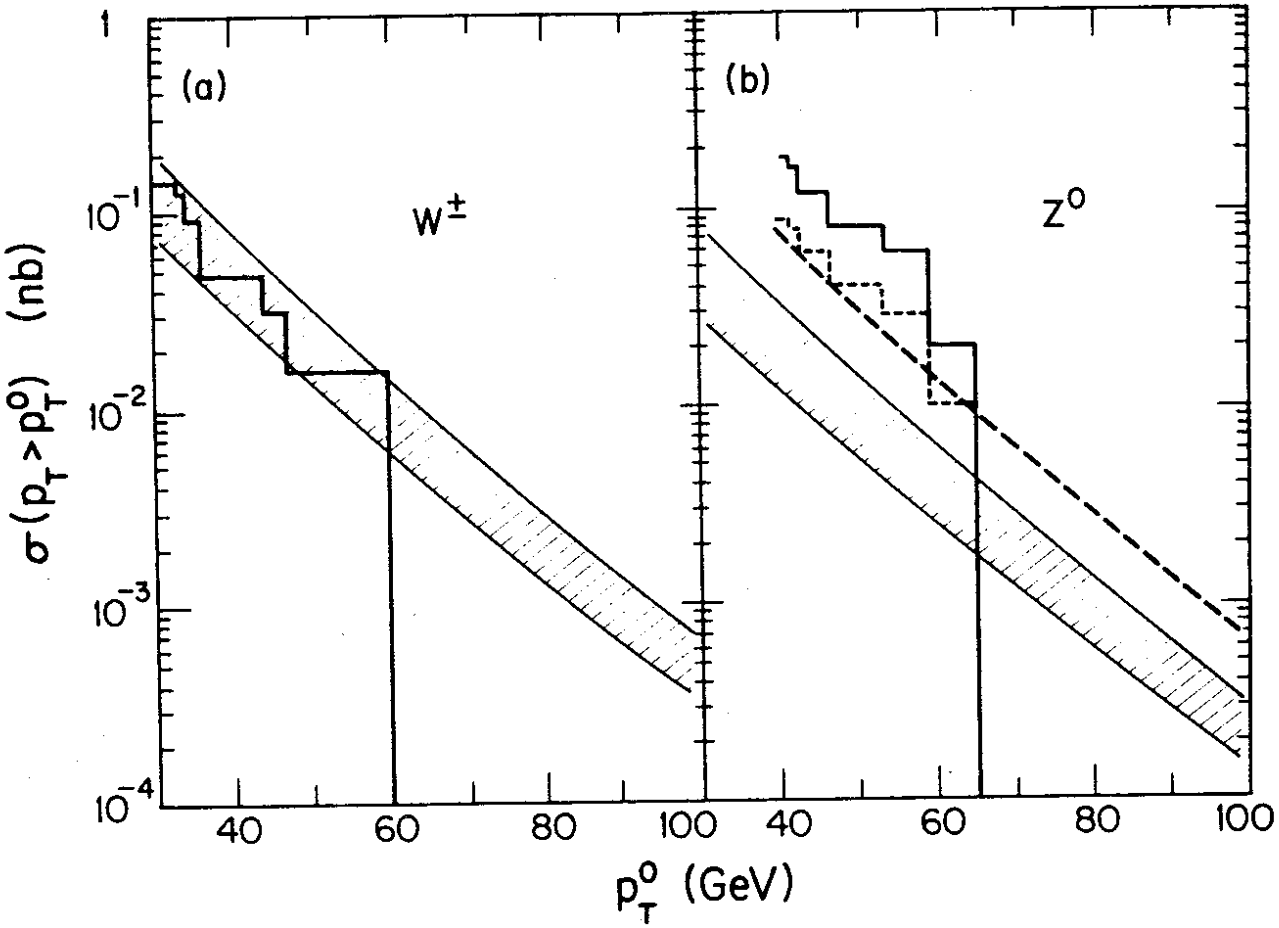

Fig. 4

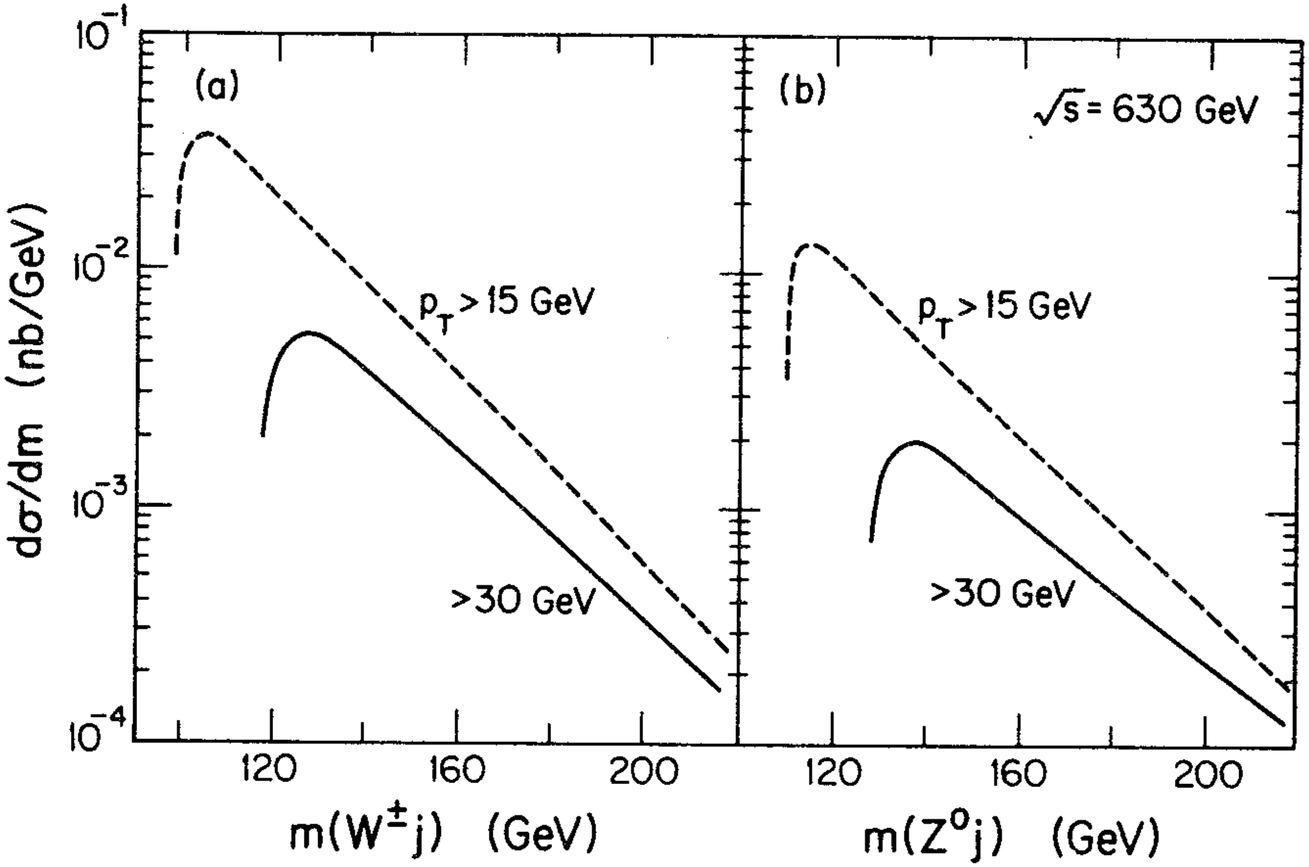
(a)
(b)
$\sqrt{s}$ = 630 GeV
p_T > 15 GeV
>30 GeV
p_T > 15 GeV
>30 GeV
dσ/dm (nb/GeV)
10^{-1}
10^{-2}
10^{-3}
10^{-4}
120
160
200
120
160
200
m($W^{\pm}$j) (GeV)
m(Z^{o}j) (GeV)

Fig. 5

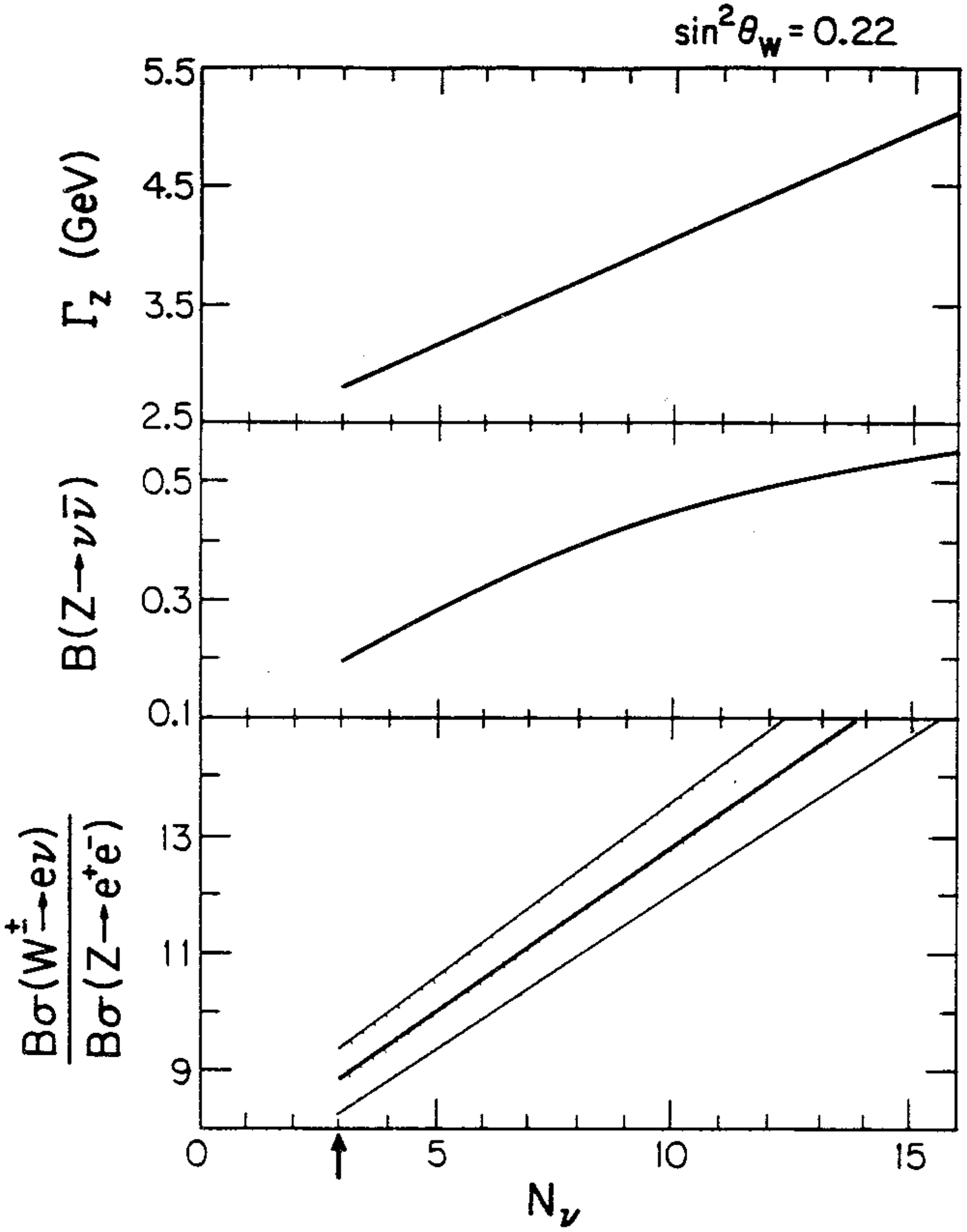

$\sin^2\theta_W = 0.22$
5.5
4.5
3.5
2.5
Γ_Z (GeV)
0.5
0.3
0.1
$B(Z \to \nu\bar{\nu})$
13
11
9
$\frac{B\sigma(W^{\pm} \to e\nu)}{B\sigma(Z \to e^+e^-)}$
0
5
10
15
N_ν

Fig. 6